



RESEARCH ARTICLE

CLASSIFICATION OF BRAIN TUMORS WITH DEEP LEARNING MODELS

Beyza Nur TÜZÜN^{1*}, Durmuş ÖZDEMİR²

^{1*} Kütahya Dumlupınar University, Institute of Graduate Education, Department of Computer Engineering, Kütahya,
b.nur.tuzun@gmail.com, ORCID: 0000-0002-8289-6263

² Kütahya Dumlupınar University, Faculty of Engineering, Department of Computer Engineering, Kütahya,
durmus.ozdemir@du.edu.tr, ORCID: 0000-0002-9543-4076

Receive Date: 05.05.2023

Accepted Date: 15.09.2023

ABSTRACT

This study aims to present a comparative analysis of existing (state-of-the-art) deep learning models to identify early detection of brain tumor disease using MRI (Magnetic Resonance Imaging) images. For this purpose, GoogleNet, Mobilenetv2, InceptionV3, and Efficientnet-b0 deep learning models were coded on the Matlab platform and used to detect and classify brain tumor disease. Classification has been carried out on the common Glioma, Meningioma, and Pituitary brain tumors. The dataset includes 7022 brain MRI images in four different classes, which are shared publicly on the Kaggle platform. The dataset was pre-processed and the models were fine-tuned, and appropriate parameter values were used. When the statistical analysis results of the deep learning models we compared were evaluated, the results of Efficientnet-b0 (%99.54), InceptionV3 (%99.47), Mobilenetv2 (%98.93), and GoogleNet (%98.25) were obtained, in the order of success. The study results are predicted to be useful in offering suggestions to medical doctors and researchers in the relevant field in their decision-making processes. In particular, it offers some advantages regarding early diagnosis of the disease, shortening the diagnosis time, and minimizing human-induced errors.

Keywords: *Deep Learning, Brain Tumor Detection, Image Classification, MRI processing*

1. INTRODUCTION

Artificial neural networks (ANN) are models that can derive and create new information by using previously learned or classified information with an artificial network structure and produce outputs that can make decisions [1]. The learning process in ANN is similar to the relationship between neurons (nerve cells) and neurons, as in the human brain, and certain adjustments are required. The first ANN cell model was developed by Warren McCulloch and Walter Pitts in 1943. They modeled a simple neural network using electrical circuits to explain how neurons in the brain work [2].

Deep learning is an artificial intelligence method that uses multi-layer artificial neural networks in the fields of image and sound processing [3]. Each layer in deep learning have more than one number of

neurons, the hidden layer; is the layer that has the most impact on learning ability [4]. Unlike machine learning, it can learn by automatically inferences from the symbols of the data in the image or sound without using external user-defined rules. Estimation accuracy rates increase according to the input data size and normalization processes [5], [6]. With the development and spread of deep learning models, studies have been carried out in many different fields, especially in the field of medicine [7], [9]. In the studies, factors such as solving the problems in the diagnosis and treatment process of time-consuming and complex diseases in the health sector, and determining how genetic variations cause disease are aimed.

The main visualization techniques used for the identification of diseases are CT (Computed Tomography) and MRI (Magnetic Resonance Imaging) imaging techniques [10]. With the CT technique, a clear image is obtained in the images of anatomical structures such as bones, but this clarity is lower in soft tissues and organs. The MR imaging technique can clearly reflect anatomical structures such as soft tissues, organs, and vessels [11]. For this reason, MRI imaging is used to detect brain tumors. In the phase of the regeneration of cells, mass or masses may occur in various parts of the body in cases caused by excessive proliferation, defects in the development, growth, and proliferation of the cell deviating from its average size, radiation exposure, genetic disorders [12]. These masses are called tumors. A brain tumor is a mass that results from the uncontrolled development and growth of brain cells within the skull [13]. Brain tumors are basically divided into benign and malignant. Benign tumors grow slowly and rarely spread. Their marginal structures can distinguish them. Malignant tumors grow and spread very quickly. They often threaten human life. Brain tumors with evolving medical imaging techniques and classification of findings in different patients are divided into two superclasses, primary and secondary, and 11 subclasses [14]. While primary brain tumor types originate from brain cells, secondary brain tumor types originate anywhere in the body and then spread to the brain. The 2016 American Association of Neurological Surgeons (AANS) classification of brain tumor types based on data from WHO (World Health Organization) is as follows [15], [16]:

I. Primary tumors of the brain

- Gliomas
- Meningioma
- Primitive neuroectodermal tumors (PNET)
- Pituitary tumors
- Pineal tumors
- Choroid plexus tumors
- Other, more benign primary tumors
- Tumors of nerves and/or nerve sheaths
- Cysts
- Other primary tumors, including skull base
- Primary Central Nervous System Lymphoma (PCNSL)

II. Metastatic brain tumors and carcinomatous meningitis

Glioma, Meningioma, and Pituitary brain tumor types commonly seen in this study were classified [17]. We also classified Brain MRI images using GoogleNet InceptionV3, MobileNetV2, and

Efficientnet-b0 deep learning models and compared the results with performance metrics for accuracy. In the study, fine-tuning and problem-oriented adaptation processes were carried out to obtain the best accuracy rate depending on parameters such as the number of training rounds and learning rate.

2. RELATED WORKS

Gürkahraman et al. [18] aimed to classify three different brain tumors (glioma, meningioma and pituitary gland tumor) using a convolutional neural network (CNN) on T1-weighted MR images and to determine the effectiveness of axial, coronal and sagittal MR sections in classification. They compared with DVM, k-NN, and Bayesian classifiers. The features existed extracted with the CNN model, and then the dataset was classified with SVM, k-NN, and Bayes classifiers. Noreen et al. [19] aimed to classify three different brain tumor MR images. In the final applications of pre-trained models, features were extracted from substrates that are different from natural images and medical images. They propose a multi-level feature extraction and merging method to solve this problem. They make changes to the Inception-v3 and DensNet201 model.

Sultan et al. [20] aimed to prove the ability of their new model to classify two different datasets with different labels. They performed classification on two separate datasets containing 3064 and 516 brain MRI images available to the public. They proposed a deep learning model based on CNN structure to classify different types of brain tumors. The second dataset aimed to differentiate between three grades of glioma, Stage 2, Stage 3, and Stage 4 tumor classes. Yerukalareddy and Pavlovskiy [21] proposed a new deep learning model for brain tumor classification in MRI images. They tested the proposed approach on two different MRI datasets and three types of brain tumors; It contains four different labels: glioma, meningioma, pituitary, and healthy. Divya et al. [22] used the ResNet50 model to classify MR brain images of tumor types such as glioma, meningioma, and pituitary. For a better result, they changed the layers and increased the number of layers from 174 layers to 181 layers. In the pieces of training, the Figshare MRI dataset consists of 3064 T1-weighted contrast-enhanced MR images of 233 patients with three different brain tumor types, including glioma, meningiomas, and pituitary tumors, containing 1426, 708, and 930 images, respectively, were utilized. Rehman et al. [23] used three convolutional neural network architectures to classify brain tumor types such as meningioma, glioma, and pituitary; Three studies were run using AlexNet, GoogLeNet, and VGGNet. The proposed studies observed that the fine-tuned VGG16 architecture achieved the highest accuracy of classification and detection, up to 98.69%. Deepak and Ameer [24] proposed the GoogleNet model to classify brain tumor types such as meningioma, glioma, and pituitary in their study. They created a system that followed a five-fold cross-validation process at the patient level on the MRI dataset from Figshare.

3. MATERIAL AND METHOD

3.1. Dataset

The dataset used in this study includes a total of 7022 brain MRI images in 4 different classes, shared openly by Masoud Nickparvar on the Kaggle platform. Examples from the dataset we used in the study are presented in Figure 1.

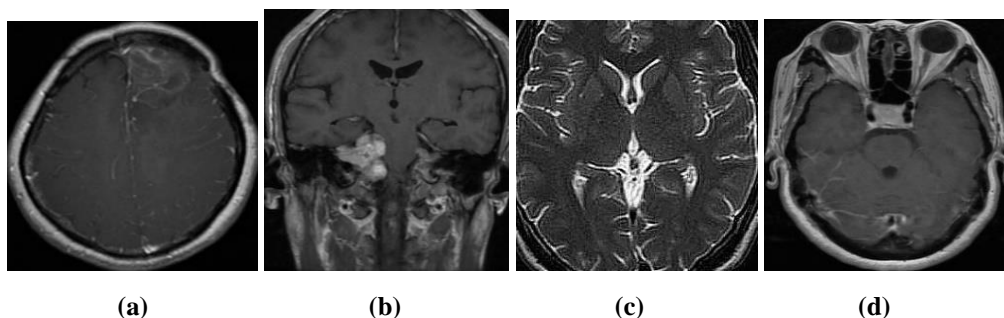


Figure 1. Examples from the data set are labeled as (a) glioma, (b) meningioma, (c) pituitary, and (d) no tumor, respectively.

Around 22% of the images were used as model tests and the rest as the training dataset. Data can be accessed from <https://www.kaggle.com/masoudnickparvar/brain-tumor-MRI-dataset> [25], [26]. The distribution of the images were Glioma (1645), Meningioma (1621), Pituitary (1757) ve No tumor (1600).

3.2. Preprocessing Stages and Fine-Tuning.

Brain MRI images were preprocessed using the OpenCV library. The endpoints in the image were found, and the margins were cropped. To apply the 45-threshold value threshold method to the images, grey coloring and blurring were made with the Gaussian Blur method. A series of erode and dilate methods were applied to eliminate small noise regions in the images equated with the Threshold method, and new images were obtained. Matlab imageDataAugmenter method RandRotation, RandXTranslation, and RandXTranslation parameters were applied in the [-20,20] rotation range before the models existed trained. Since the models use the RGB pixel color type, the images stand converted to RGB type. Unprocessed and preprocessed images in the data set used in the study were presented in Figure2.

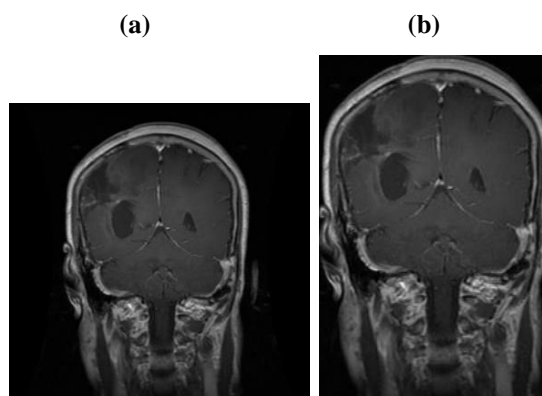


Figure 2. (a) Unprocessed image (b) Preprocessed image

3.3. Experimental Settings.

The blue markers in Figure 3 presented in show the space that the models occupy on the disk and the memory sizes. As the size of the models increases, the number of layers also increases. According to this figure, smaller-sized models were selected and their performances were compared in this study. The exact estimation and training iteration times depend on the hardware you use and the mini-batch size. Before the training phase the last fully connected layer (Fully Connected Layer) and classification (Classification Layer) layers were substituted with new ones to classify brain tumors. The training was assumed out in the Matlab R2021a application environment. A computer with 2.4GHz Intel(R)Core™ i7-3630QM CPU and Nvidia 950M GPU with 16 Ram was utilized for hardware. The parameter settings we applied in our model during the training phase are presented in Table 1.

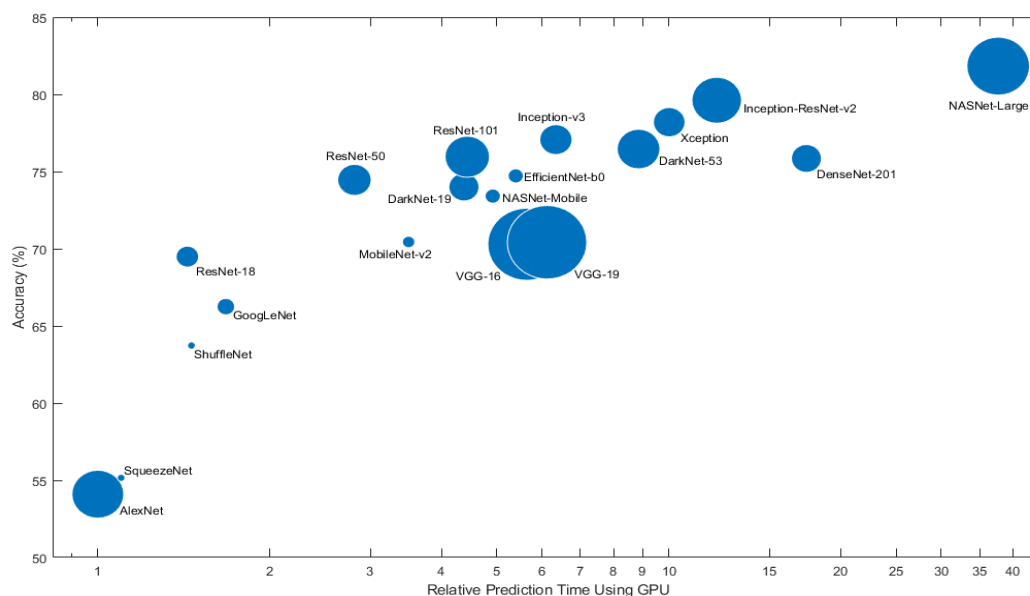


Figure 3. The relative training estimation time of models on GPU processor.

Table 1. Parameter Values

Epochs	30, 50, 100
Momentum	0.9
InitialLearnRate	0.1
Classes	4
Mini batch	16
Optimizer	'sgdm'
Verbose	False

L2Regularization	0.0001
GradientThresoldMethot	L2norm
GradientThresold	0.1
Learning rate schedule	Piecewise
Learning rate drop period	10
Learning rate drop factor	0.1

3.4. Evaluation with Performance Metrics.

The trained model is tested at the end of the training with different data reserved for the test, and a Confusion matrix is created with the results obtained. In this study we use the True Positive(TP), True Negative(TN), False Positive(FP), and False Negative(FN) performance metrics [27].

$$Accuracy = \frac{TP+TN}{TP+FN+TN+FP} \quad (1)$$

$$Recall = \frac{TP}{TP+FN} \quad (2)$$

$$Precision = \frac{TP}{TP+FP} \quad (3)$$

$$F1\ Score = 2 \times \frac{Precision \times Recall}{Precision + Recall} \quad (4)$$

The pieces of training were carried out with 100, 50, and 30 epochs, and the test results of the pieces of training were compared. In models trained with 100 epochs, the learn rate decreased by 0.01 every 10 epochs; in the last ten epochs, training was realized with a 1e-10 learn rate. Models trained with 50 epochs ended up with a learning rate of 1e-5, with the learn rate decreasing by 0.01 every ten epochs. Pieces of training made with 30 epochs started with 0.1 initial learning rate, and again in 10 epochs, the learning rate was reduced by 0.01 and ended with a learning rate of 0.0001. The accuracy, recall, precision, and f1 score values that change according to the test results of the models are shown in Table 2 below.

Table 2. The Test Results According to The Number of Training Epoch

Model	Epoch	Accuracy (%)	Recall (%)	Precision (%)	F1 Score (%)
GoogleNet	30	95.12	94.82	94.88	94.85
GoogleNet	50	98.93	98.84	98.87	98.86
GoogleNet	100	98.25	98.10	98.14	98.12
MobileNetV2	30	95.19	94.92	95.07	95
MobileNetV2	50	98.86	98.76	98.79	98.77
MobileNetV2	100	98.93	98.87	98.9	98.88
Efficientnet-b0	30	95.27	94.95	95.22	95.08

Efficientnet-b0	50	99.08	99.01	99.07	99.04
Efficientnet-b0	100	99.54	99.52	99.54	99.53
InceptionV3	30	96.80	96.56	96.76	96.66
InceptionV3	50	99.38	99.34	99.36	99.35
InceptionV3	100	99.47	99.42	99.45	99.43

As seen in Table 2, the training of the models, EfficientNet-b0, with 100 epochs, yielded the most successful results in the testing phase.

4. FINDINGS AND DISCUSSION

After Results of this study were presented to prevent overfitting, that is, excessive learning, while training epochs with piecewise different learn rate values with the piecewise parameter. However, parts trained with a high-value learn rate may not be fully trained. If it is low, the training may have slowed down, and the training period may have been prolonged. For this reason, retraining was done with different epoch values, and the results were compared. Among the GoogleNet, InceptionV3, MobileNetV2, and EfficientNet-b0 models, The best result values were obtained with the Efficientnet-b0 model, which was trained with 100 epochs. 99.54% accuracy, 99.52% recall, 99.54% precision and 99.53% f1-score values were obtained. However, results close to these values were obtained with other models as well. The Confusion Matrix of the EfficientNet-b0 model was given in Figure 4.

The results obtained from the test data of the model are as follows, respectively. The accuracy value for glioma-type tumors was obtained as 99.5%. In the glioma test data, 2 MRI images were incorrectly identified as meningioma, and 1 MRI image was defined as healthy (no tumor). The error rate value was found to be 1%. The predictive accuracy of meningioma type, which is one of the tumor types, was found to be 100%. A predictive accuracy of 99.3% was obtained in another tumor type, the pituitary. In the pituitary test results, 2 MRI images were wrong with an error rate of 0.7% and were defined as meningioma. As a result, the prediction accuracy for healthy MRI images of the brain is 99.8%. Among the healthy test data (no-tumor), 1 MRI brain image was misidentified as meningioma, and the error rate was 0.2%.

		Confusion Matrix				
Output Class	glioma	297 22.7%	0 0.0%	0 0.0%	0 0.0%	100% 0.0%
	meningioma	2 0.2%	306 23.3%	1 0.1%	2 0.2%	98.4% 1.6%
	notumor	1 0.1%	0 0.0%	404 30.8%	0 0.0%	99.8% 0.2%
	pituitary	0 0.0%	0 0.0%	0 0.0%	298 22.7%	100% 0.0%
		99.0% 1.0%	100% 0.0%	99.8% 0.2%	99.3% 0.7%	99.5% 0.5%
		glioma	meningioma	notumor	pituitary	
		Target Class				

Figure 4. The Confusion Matrix of the EfficientNet-b0 model

Noreen et al. made changes in the InceptionV3 and DenseNet201 models in their study and obtained new models. These two new CNN models achieved an accuracy rate of 99.34% in the InceptionV3 model. When this result is compared with the training results made with the InceptionV3 model we used in this study, the test accuracy result of the training performed by setting 30 epochs was below the value obtained. However, in this study, it was observed that the test results of the pieces of training we performed with 50 and 100 epochs were more successful than the 99.34% accuracy rate. Again, Noreen et al. obtained an accuracy rate of 99.51% with the DenseNet201 model. In the Efficientnet-b0 model we suggested in the study, we achieved a test accuracy of 99.54% when 100 epochs were used, and it was observed that this ratio was more successful than the accuracy of the DenseNet201 model.

Deepak and Ameer [24] also achieved an accuracy rate of 98% with GoogleNet in their study. But in our study, as a result of the pieces of training carried out with GoogleNet, the accuracy rate of the training made by setting 30 epochs remained below this rate. However, it was observed that the test accuracy rates of the pieces of training performed by setting 50 and 100 epochs were more successful.

5. CONCLUSIONS AND SUGGESTION

As a result, this study uses deep learning models GoogleNet, InceptionV3, MobileNetV2, and Efficientnet-b0; It has been observed to be successful in classifying and detecting glioma meningioma and pituitary brain tumor types. The images and classes in the data set can be increased in future studies. Today, 3D techniques have begun to be used. Since this imaging method will increase in the future, it is recommended to work with these 3D images. This study used four deep learning models with faster training time. Apart from the four models used in the study, studies can be carried out with

other models or by creating a new model. By reusing the deep learning models used in the study, Apart from brain tumor types, classification and detection studies can be performed with MRI images of different disease type.

ACKNOWLEDGEMENT

The authors thank the reviewers for their valuable comments and suggestions, which improved the clarity and scope of the article.

ETHICAL APPROVAL

This study was carried out as part of the master thesis [ID: 720611] prepared by Beyza Nur TUZUN under the supervision of Assoc. Prof. Dr. Durmus OZDEMIR.

REFERENCES

- [1] Copeland, B. J., and Proudfoot, D. (2007). Artificial intelligence. *Philosophy of Psychology and Cognitive Science*, 429–482. <https://doi.org/10.1016/b978-044451540-7/50032-3>
- [2] Macukow, B. (2016). Neural Networks – State of Art, Brief History, Basic Models and Architecture. *Computer Information Systems and Industrial Management*, 3–14. https://doi.org/10.1007/978-3-319-45378-1_1
- [3] Seyyarer, E., Uçkan, T., Hark, C., Ayata, F., İnan, M., and Karcı, A. (2019). Applications and Comparisons of Optimization Algorithms Used in Convolutional Neural Networks. 2019 International Artificial Intelligence and Data Processing Symposium (IDAP). <https://doi.org/10.1109/idap.2019.8875929>
- [4] Kartal, M., and Duman, O. (2019). Ship Detection from Optical Satellite Images with Deep Learning. 2019 9th International Conference on Recent Advances in Space Technologies (RAST). <https://doi.org/10.1109/rast.2019.8767844>
- [5] Şeker, A., Diri, B., and Balık, H. H. (2017). Derin Öğrenme Yöntemleri Ve Uygulamaları Hakkında Bir İnceleme. *Gazi Mühendislik Bilimleri Dergisi*, 3(3), 47–64. Retrieved from <https://dergipark.org.tr/tr/pub/gmbd/issue/31064/372661>
- [6] Alzubaidi, L., Zhang, J., Humaidi, A. J., Al-Dujaili, A., Duan, Y., Al-Shamma, O., Fadhel, M. A., Al-Amidie, M., and Farhan, L. (2021). Review of deep learning: concepts, CNN architectures, challenges, applications, future directions. *Journal of Big Data*, 8(1). <https://doi.org/10.1186/s40537-021-00444-8>

- [7] Özdemir, D., and Arslan, N. N. (2022). Analysis of Deep Transfer Learning Methods for Early Diagnosis of the Covid-19 Disease with Chest X-ray Images. *Düzce Üniversitesi Bilim ve Teknoloji Dergisi*, 628–640. <https://doi.org/10.29130/dubited.976118>
- [8] Ravi, D., Wong, C., Deligianni, F., Berthelot, M., Andreu-Perez, J., Lo, B., and Yang, G.-Z. (2017). Deep Learning for Health Informatics. *IEEE Journal of Biomedical and Health Informatics*, 21(1), 4–21. <https://doi.org/10.1109/jbhi.2016.2636665>
- [9] Adeli, E., Rekik, I., Park, S. H., and Shen, D. (2020). Editorial: Predictive Intelligence in Biomedical and Health Informatics. *IEEE Journal of Biomedical and Health Informatics*, 24(2), 333–335. <https://doi.org/10.1109/jbhi.2019.2962852>
- [10] Kumamaru, K. K., Machitori, A., Koba, R., Ijichi, S., Nakajima, Y., and Aoki, S. (2018). Global and Japanese regional variations in radiologist potential workload for computed tomography and magnetic resonance imaging examinations. *Japanese Journal of Radiology*, 36(4), 273–281. <https://doi.org/10.1007/s11604-018-0724-5>
- [11] Yang, W., and Liu, J. (2013). Research and development of medical image fusion. <https://doi.org/10.1109/icmipe.2013.6864557>
- [12] Srikanth, B., and Venkata Suryanarayana, S. (2021). Multi-Class classification of brain tumor images using data augmentation with deep neural network. *Materials Today: Proceedings*. <https://doi.org/10.1016/j.matpr.2021.01.601>
- [13] Lavanyadevi, R., Machakowsalya, M., Nivethitha, J., and Kumar, A. N. (2017). Brain tumor classification and segmentation in MRI images using PNN. 2017 IEEE International Conference on Electrical, Instrumentation and Communication Engineering (ICEICE). <https://doi.org/10.1109/iceice.2017.8191888>
- [14] Julià-Sapé, M., Griffiths, J. R., Tate, R. A., Howe, F. A., Acosta, D., Postma, G., Underwood J., Majós C., and Arús, C. (2015). Classification of brain tumours from MR spectra: the INTERPRET collaboration and its outcomes. *NMR in Biomedicine*, 28(12), 1772–1787. <https://doi.org/10.1002/nbm.3439>
- [15] Louis, D. N., Perry, A., Wesseling, P., Brat, D. J., Cree, I. A., Figarella-Branger, D., Hawkins, C., Ng, H. K., Pfister, S. M., Reifenberger, G., Soffietti, R., von Deimling, A., and Ellison, D. W. (2021). The 2021 WHO Classification of Tumors of the Central Nervous System: a summary. *Neuro-Oncology*, 23(8). <https://doi.org/10.1093/neuonc/noab106>
- [16] Villa, C., Miquel, C., Mosses, D., Bernier, M., and Di Stefano, A. L. (2018). The 2016 World Health Organization classification of tumours of the central nervous system. *La Presse Médicale*, 47(11-12), e187–e200. <https://doi.org/10.1016/j.lpm.2018.04.015>

- [17] Zhou, Z., Wu, S., Chang, K.-J., Chen, W.-R., Chen, Y.-S., Kuo, W.-H., Lin, C.-C., and Tsui, P.-H. (2015). Classification of Benign and Malignant Breast Tumors in Ultrasound Images with Posterior Acoustic Shadowing Using Half-Contour Features. *Journal of Medical and Biological Engineering*, 35(2), 178–187. <https://doi.org/10.1007/s40846-015-0031-x>
- [18] Gürkahraman, K., and Karakış, R. (2021). Veri çoğaltma kullanılarak derin öğrenme ile beyin tümörlerinin sınıflandırılması. *Journal of the Faculty of Engineering and Architecture of Gazi University*, 36(2), 997–1012. <https://doi.org/10.17341/gazimmfd.762056>
- [19] Noreen, N., Palaniappan, S., Qayyum, A., Ahmad, I., Imran, M., and Shoaib, M. (2020). A Deep Learning Model Based on Concatenation Approach for the Diagnosis of Brain Tumor. *IEEE Access*, 8, 55135–55144. <https://doi.org/10.1109/access.2020.2978629>
- [20] Sultan, H. H., Salem, N. M., and Al-Atabany, W. (2019). Multi-Classification of Brain Tumor Images Using Deep Neural Network. *IEEE Access*, 7, 69215–69225. <https://doi.org/10.1109/access.2019.2919122>
- [21] Yerukalareddy, D. R., and Pavlovskiy, E. N. (2021). Brain Tumor Classification based on MR Images using GAN as a Pre-Trained Model. 2021 IEEE Ural-Siberian Conference on Computational Technologies in Cognitive Science, Genomics and Biomedicine (CSGB), 380–384. IEEE.
- [22] Divya, S., Padma Suresh, L., and John, A. (2020). A Deep Transfer Learning framework for Multi Class Brain Tumor Classification using MRI. 2020 2nd International Conference on Advances in Computing, Communication Control and Networking (ICACCCN). <https://doi.org/10.1109/icacccn51052.2020.9362908>.
- [23] Rehman, A., Naz, S., Razzak, M. I., Akram, F., and Imran, M. (2019). A Deep Learning-Based Framework for Automatic Brain Tumors Classification Using Transfer Learning. *Circuits, Systems, and Signal Processing*, 39(2), 757–775. <https://doi.org/10.1007/s00034-019-01246-3>
- [24] Deepak, S., and Ameer, P. M. (2019). Brain tumor classification using deep CNN features via transfer learning. *Computers in Biology and Medicine*, 111, 103345. <https://doi.org/10.1016/j.combiomed.2019.103345>
- [25] Cheng, J. (2017, April 2). brain tumor dataset. Retrieved from Figshare website: https://figshare.com/articles/dataset/brain_tumor_dataset/1512427
- [26] Nickparvar, M. (2021). Brain Tumor MRI Dataset. Retrieved from Kaggle website: <https://www.kaggle.com/datasets/masoudnickparvar/brain-tumor-mri-dataset/metadata>
- [27] Luque, A., Carrasco, A., Martín, A., and de las Heras, A. (2019). The impact of class imbalance in classification performance metrics based on the binary confusion matrix. *Pattern Recognition*, 91, 216–231. <https://doi.org/10.1016/j.patcog.2019.02.023>